Supporting Information

Li et al. 10.1073/pnas.1016884108

SI Materials and Methods

Plant Materials. The minimal *Mutator* line consists of one fully active *MuDR* element at position 1 (p1) on chromosome 2L (here simply referred to as "*MuDR*," because this work deals exclusively with *MuDR* at this position) (1). *Muk* is a derivative version of *MuDR* as described previously (2). Activity was monitored in seeds via excisions of a nonautonomous *Mu1* element inserted into the *a1-mum2* color gene (1). Plants carrying *MuDR* and *Muk* in the first generation are referred to as F1 plants. F1 individuals were generated from the cross between a plant heterozygous for *Muk* and a plant carrying an active *MuDR*(*p1*) element, *Muk*/− × *MuDR*/−. Lines containing stably silenced *MuDR* were established by test-crossing an F1 plant carrying both *MuDR* and *Muk* to an *a1-mum2* tester, which carries *Mu1* at *a1-mum2* but which lacks both *MuDR* and *Muk*. Progeny plants carrying stably silenced *MuDR* elements without *Muk* (F2 plants) were then recurrently back-crossed to the *a1-mum2* parent line for six generations. No evidence for activity (somatic excision of the reporter *Mu1* element from the *a1-mum2* color gene) was observed in this line for at least four generations. The resulting silenced *MuDR*(*p1*) elements are referred to as stably silenced *MuDR* elements.

To examine the effects of mutations in *lbl1* on *Muk*-induced silencing of *MuDR*, we constructed lines that segregated for *MuDR*, *Muk*, and the reference allele of *lbl1*, *lbl1-ref*. This allele was used because its relatively mild phenotype made it possible to unambiguously determine the order of the first few leaves, which would be more difficult to do with a stronger allele because of its dramatic effect on leaf morphology. A plant carrying *lbl-ref* was crossed as a homozygote to a plant that was homozygous for *Muk* and to a plant that was heterozygous for *MuDR* at position 1 on chromosome 2L. A plant that was heterozygous for both *Muk* and *lbl-ref* was then crossed to a plant that was heterozygous for *MuDR* and *lbl1-ref*. The resulting progeny were then examined for the *lbl1-ref* phenotype and genotyped for both *Muk* and *MuDR*. Bisulfite sequencing analysis was then performed on immature leaf 3 of three mutant plants and two wild-type siblings. Leaf 3 was examined because we had previously determined that TIRA in leaf 3 of F1 *MuDR;Muk* plants is invariably methylated, and in both the *lbl1* mutant and wild-type plants examined here, leaf 3 was morphologically juvenile.

In a similar way, we constructed lines that segregated for *MuDR*, *Muk* in the *Corngrass1* mutant, and wild-type siblings. Bisulfite sequencing analysis and RT-PCR were performed on immature leaf 6 and leaf 10 of mutant and wild-type siblings, respectively. In the *Cg1* mutant plants examined here, leaf 10 expressed both juvenile and adult traits.

Tissue Sampling. All plants used in the bisulfite sequencing and chromatin immunoprecipitation (ChIP) experiments illustrated in Figs. 1 and 2 were genotyped individually; leaves with the same genotype were pooled from multiple, different genotyped individuals from four independent families, two of which were derived from a cross that used *Muk* as a female and two of which used *Muk* as a male. The visible portion of each immature (developing) leaf blade was harvested soon after it emerged from the leaf whorl, when it was ≈6 cm long. Leaves were removed sequentially from the same plants as they matured. Mature leaves were harvested when they were fully expanded. Only leaf blades (not sheaths) were collected. Plants were dissected to collect immature tassels that were ≈1 cm long. Immature ears were harvested once they were ≈6 cm long. Shoot apex tissue included the shoot apical meristem along with the youngest leaf primordia surrounding the shoot apical meristem from 2-wk-old seedling. Samples used for the bisulfite sequencing analysis and the ChIP assays were from the same sample pools. All experiments were repeated with at least three biologically independent sample pools.

Southern Blotting. Genotyped DNA was used in Southern blotting. Briefly, 10 μg of DNA was digested with a fourfold excess of restriction enzyme for a minimum of 2 h, blotted, and probed with an internal portion of *Mu1* as previously described (1).

Identification of Maize Orthologs of *Arabidopsis* Genes. The maize *leafbladeless1* (*lbl1*) gene has been previously identified as the closest maize homolog and likely ortholog of *SGS3* (3). To confirm the hypothesis that *lbl1* is the ortholog of *SGS3*, the published *lbl1* sequence was used as a query in a BLASTn search with an *e* value cutoff of 0.01 to maize and *Arabidopsis*. The only significant hit in *Arabidopsis* was *SGS3*. There were two significant hits in maize, *lbl1* and a pseudogene fragment of *lbl1* that is unlikely to produce a functional product. Thus, we concluded that *lbl1* is the likely ortholog of *SGS3* in maize. A similar search was performed to identify the maize homolog of *AGO7*, using *Arabidopsis AGO7* as a query sequence in a search of the complete draft of the maize genome with an *e* value cutoff of 0.001. In this case, only one maize sequence with high homology (65% identity over 2.7 kb) was identified. This sequence encodes a protein designated *ragged seedling2* (*rgd2*; NCBI accession no. ACX48911.1). BLAST searching this protein against *Arabidopsis* revealed that AGO7 is the most similar protein in *Arabidopsis* to this maize protein, as has been recently demonstrated (4). A similar analysis was performed with *Arabidopsis RDR6*. In this case, however, there were five maize genes that were equally distant from RDR6, four nearly (>95%) identical paralogs on chromosome 9 (GRMZM2G347931, GRMZM2G331040, GRMZM2G357825, and GRMZM2G456682) and one additional paralog on chromosome 3 (GRMZM2G14520, designated *rdr102* in ChromDB). Of these five paralogs, only the paralog on chromosome 3 had a match to any expressed sequence tags or full-length cDNAs, so our RT-PCR experiments focused on this gene. The maize homolog of *MET1*, *Zmet1*/*dmt101*, was obtained from ChromDB (http://www.chromdb.org/). Although there are at least two homologs of the DNA glycosylases *ROS1* and *DME1* in maize, one of them, *dng101* from ChromDB, had the best EST support, so our analysis focused on this gene. Sequence for the maize homolog of *ARF3* was as previously described (3).

RNA Isolation and RT-PCR. RNA was isolated with TRIzol Reagent (Invitrogen) and the RT procedure was carried out by using SuperScript III Reverse Transcriptase (Invitrogen). Primers used in PCR amplification for *mudrA* and *aat* genes were as described previously (5). All primer sequences are provided in Table S1.

ChIP. ChIP was carried out as described previously (6, 7) with some modifications. Briefly, a total of ≈2 g of leaves or immature ears from at least 10 plants was harvested and fixed with 1% formaldehyde. For each sample, genomic DNA was sheared by sonication six times. For detection of the histone marks associated with *MuDR*, the following quantities of antibodies specific to the following modified histones were added to precleared chromatin mixtures of each sample: 3 μL of trimethylated H3K27 (Active Motif), 10 μL of dimethylated H3K27 (Millipore), 10 μL of dimethylated H3K9 (Millipore), 10 μL of trimethylated H3K4 (Millipore), or 10 μL of H3Ac (Millipore). Chromatin was reverse cross-linked. ChIP DNA was purified and dissolved in 20 μL of

TE buffer. PCR was performed with TaKaRa Ex Taq (TaKaRa Bio) in 25 μL with 1 μL of immunoprecipitated DNA. PCR conditions were as follows: 94 °C for 4 min; 33–36 cycles of 94 °C for 30 s, 57 °C for 30 s, and 72 °C for 30 s; and 72 °C for 10 min. Primers were designed in such a way that one primer was in the sequence flanking the insertion of *MuDR* into position 1 adjacent to TIRA and one primer was in the element itself.

The following primers were used in ChIP assays: actinF and actinR for *actin*, copiaF and copiaR for *copia*; TIRAR and TIRAUTRR for TIRA; and 5′AflankF1 and 5′AflankR1 for sequences flanking TIRA. The sequences of these primers are provided in Table S1. Qualitative data were obtained by comparing amplification from the gene of interest with that from control amplifications from the same ChIP sample. Controls included input DNA, *actin*, and *copia*.

Real-Time PCR Analysis. Quantitative PCR was performed by using FastStart Universal SYBR Green Master (ROX) (Roche) in a 25-μl PCR according to the manufacturer's instructions. ChIP PCR was carried out in 96-well optical reaction plates heated to 95 °C for 10 min, followed by 40 cycles of denaturation for 30 s at 95 °C, annealing for 45 s at 60 °C, and extension for 30 s at 72 °C. Technical triplicates were carried out for each sample. Quantifications were normalized to that of *actin1* or *copia*, then to the value of the active *MuDR* plant, which was arbitrarily fixed to 1. For quantification of expression of the *lbl1* gene, PCR annealing temperature was set at 61 °C and *actin1* was used as control sequence. Relative fold change was determined by using the comparative C_T method (8) normalized to control sequences. For each quantification, a melt curve was generated at the end of the amplification experiment to ensure a pure amplification of the product.

Genomic Bisulfite Sequencing. Genomic DNA was isolated as previously described (9). Two micrograms of genomic DNA from the appropriate genotype was digested with restriction enzymes that cut just outside of the region of interest. Bisulfite conversion was performed with an EpiTect Bisulfite kit (Qiagen). PCR fragments from TIRA were amplified by using TIRAmF6 and TIRAR3. The internal region between the *mudrA* and *mudrB* genes was used as control for bisulfite treatment using primers DrintF1 and DrintR1. These sequences were invariably unmethylated in all samples examined, providing a consistent control for bisulfite conversion efficiency. PCR product was purified and cloned with a CloneJET PCR Cloning Kit (Fermentas), and 10 independent clones were sequenced from each sample. The resulting sequences were analyzed with kismeth (http://katahdin.mssm.edu/kismeth/revpage.pl) (10).

Double-Stranded RNA (dsRNA) Assay. dsRNA analysis was performed as described previously (2).

1. Chomet P, Lisch D, Hardeman KJ, Chandler VL, Freeling M (1991) Identification of a regulatory transposon that controls the *Mutator* transposable element system in maize. *Genetics* 129:261–270.
2. Slotkin RK, Freeling M, Lisch D (2005) Heritable transposon silencing initiated by a naturally occurring transposon inverted duplication. *Nat Genet* 37:641–644.
3. Nogueira FTS, Madi S, Chitwood DH, Juarez MT, Timmermans MCP (2007) Two small regulatory RNAs establish opposing fates of a developmental axis. *Genes Dev* 21: 750–755.
4. Douglas RN, et al. (2010) *ragged seedling2* Encodes an ARGONAUTE7-like protein required for mediolateral expansion, but not dorsiventrality, of maize leaves. *Plant Cell* 22:1441–1451.
5. Woodhouse MR, Freeling M, Lisch D (2006) Initiation, establishment, and maintenance of heritable *MuDR* transposon silencing in maize are mediated by distinct factors. *PLoS Biol* 4:e339.
6. Gendrel AV, Lippman Z, Yordan C, Colot V, Martienssen RA (2002) Dependence of heterochromatic histone H3 methylation patterns on the *Arabidopsis* gene *DDM1*. *Science* 297:1871–1873.
7. Haring M, et al. (2007) Chromatin immunoprecipitation: Optimization, quantitative analysis and data normalization. *Plant Methods* 3:11.
8. Schmittgen TD, Livak KJ (2008) Analyzing real-time PCR data by the comparative C_T method. *Nat Protoc* 3:1101–1108.
9. Lisch D, Chomet P, Freeling M (1995) Genetic characterization of the *Mutator* system in maize: Behavior and regulation of *Mu* transposons in a minimal line. *Genetics* 139: 1777–1796.
10. Gruntman E, et al. (2008) Kismeth: Analyzer of plant methylation states through bisulfite sequencing. *BMC Bioinformatics* 9:371.

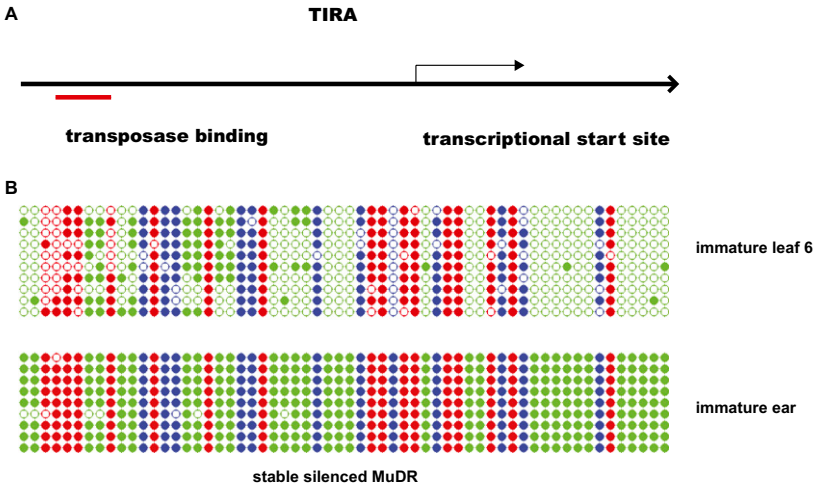

Fig. S1. DNA methylation of stably silenced TIRA in various tissues. (*A*) A diagram of TIRA showing the transposase binding site and the transcriptional start site within the terminal inverted repeat. (*B*) A comparison of TIRA methylation in stably silenced *MuDR* elements in immature leaf 6 and immature ear tissue. Ten individual clones were sequenced from each amplification of bisulfite-treated tissue. The cytosines in different sequence contexts are represented by different colors (red, CG; blue, CHG; green, CHH, where H = A, C, or T). ○, Unmethylated cytosines; ●, methylated cytosines.

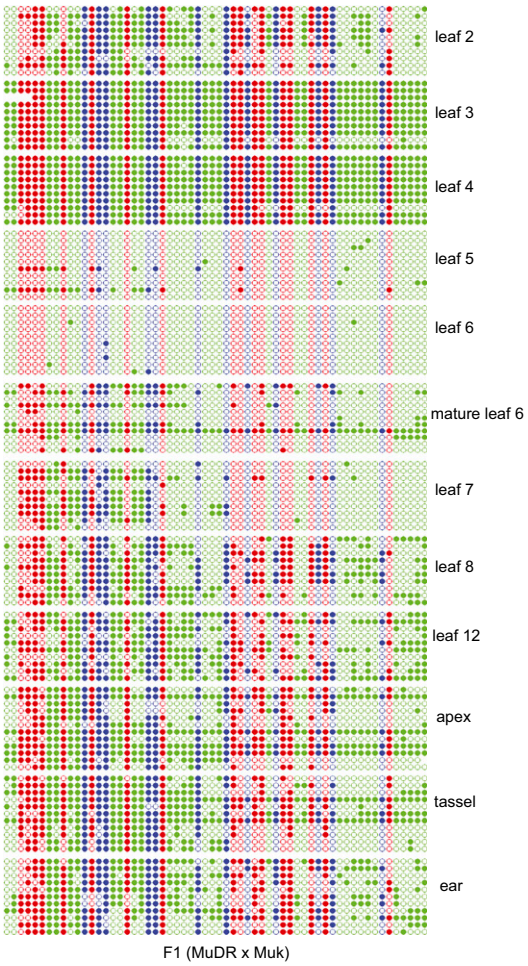

Fig. S2. DNA methylation patterns in TIRA in different tissues of F1 plants. With the exception of mature leaf 6, all leaf tissue was from young leaves. The cytosines in different sequence contexts are represented by different colors (red, CG; blue, CHG; green, CHH, where H = A, C, or T). ○, Unmethylated cytosines; ●, methylated cytosines.

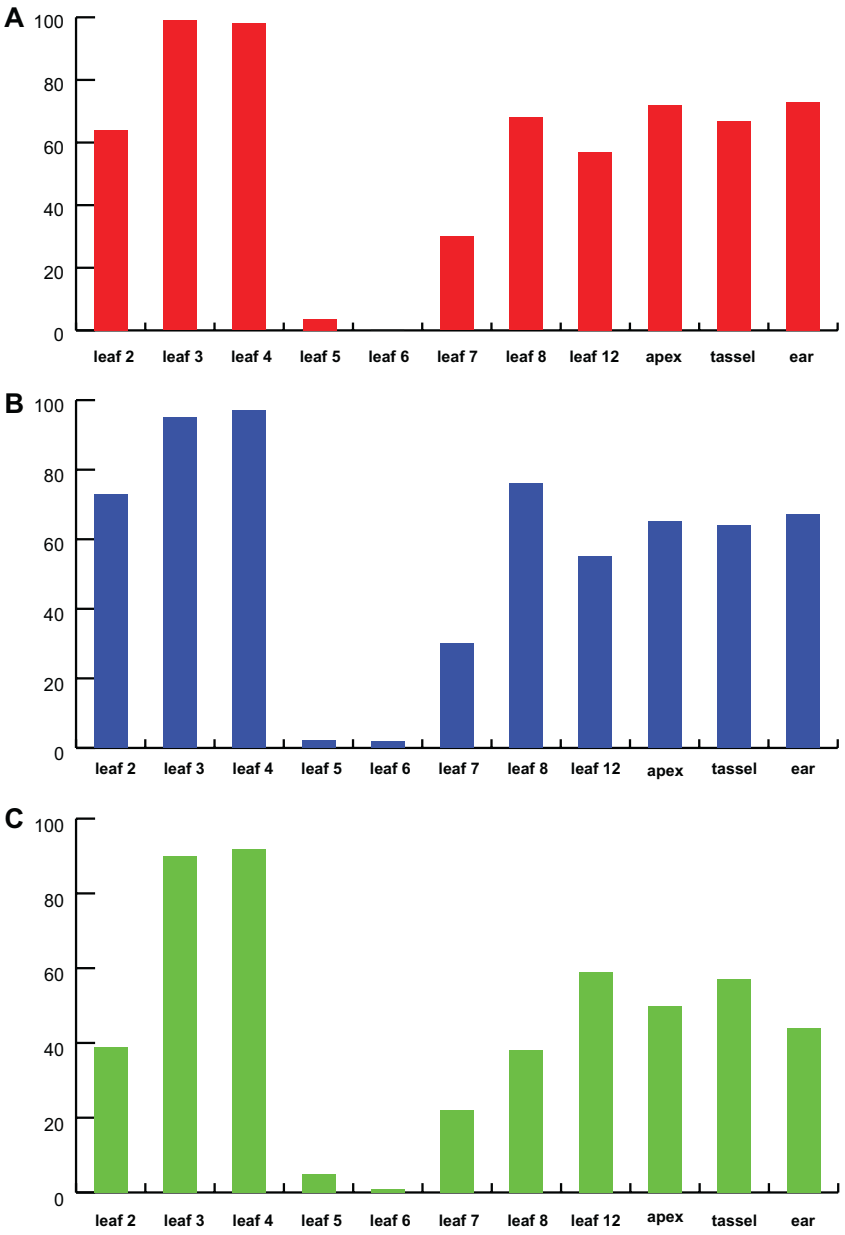

Fig. S3. Percentage of cytosines methylated in TIRA in various tissues of F1 plants. (*A*) CG methylation. (*B*) CHG methylation. (*C*) CHH methylation. H = A, C, or T.

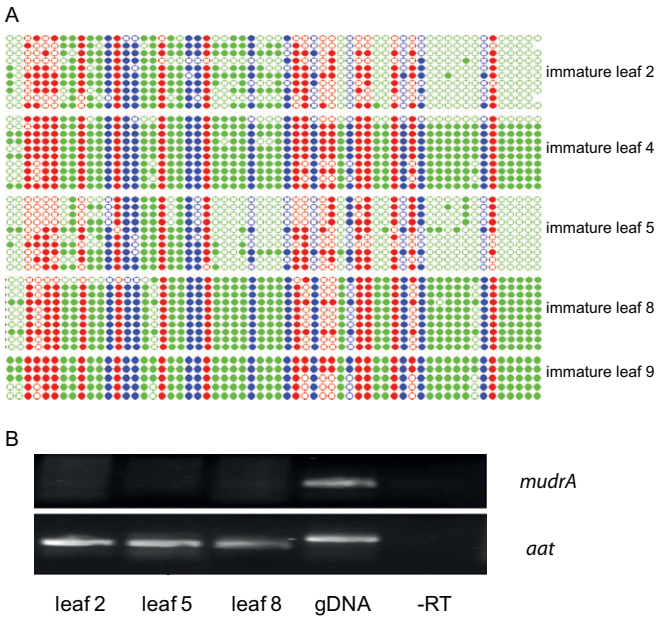

Fig. S4. (*A*) A comparison of TIRA methylation in *MuDR* in F2 plants in which the silenced *MuDR* has segregated away from *Muk* in various immature leaves. (*B*) RT-PCR detecting *mudrA* transcript in various leaves of F2 plants.

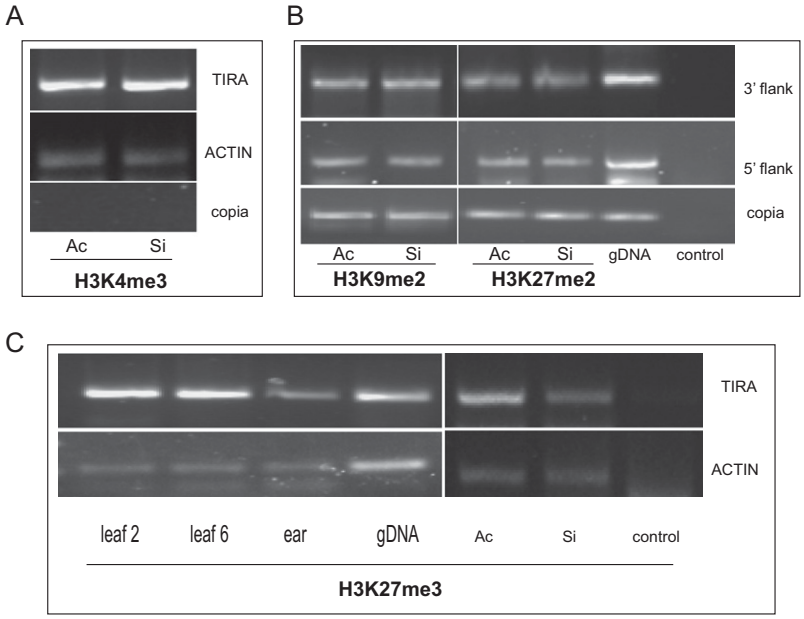

Fig. S5. Additional ChIP analysis. (*A*) ChIP analysis of enrichment of H3K4me3 at TIRA in leaf 6 in active and stably silenced *MuDR* elements. (*B*) ChIP analysis of enrichment of H3K9me2 and H3K27me2 in sequences immediately adjacent to TIRA outside of the transposon (5′ flank) and in sequences within the transposon but 3′ to the *mudrA* gene (3′ flank). (*C*) ChIP analysis of enrichment of H3K27me3 in TIRA in different tissues of F1 plants and in leaf 6 of active or stably silenced *MuDR* elements.

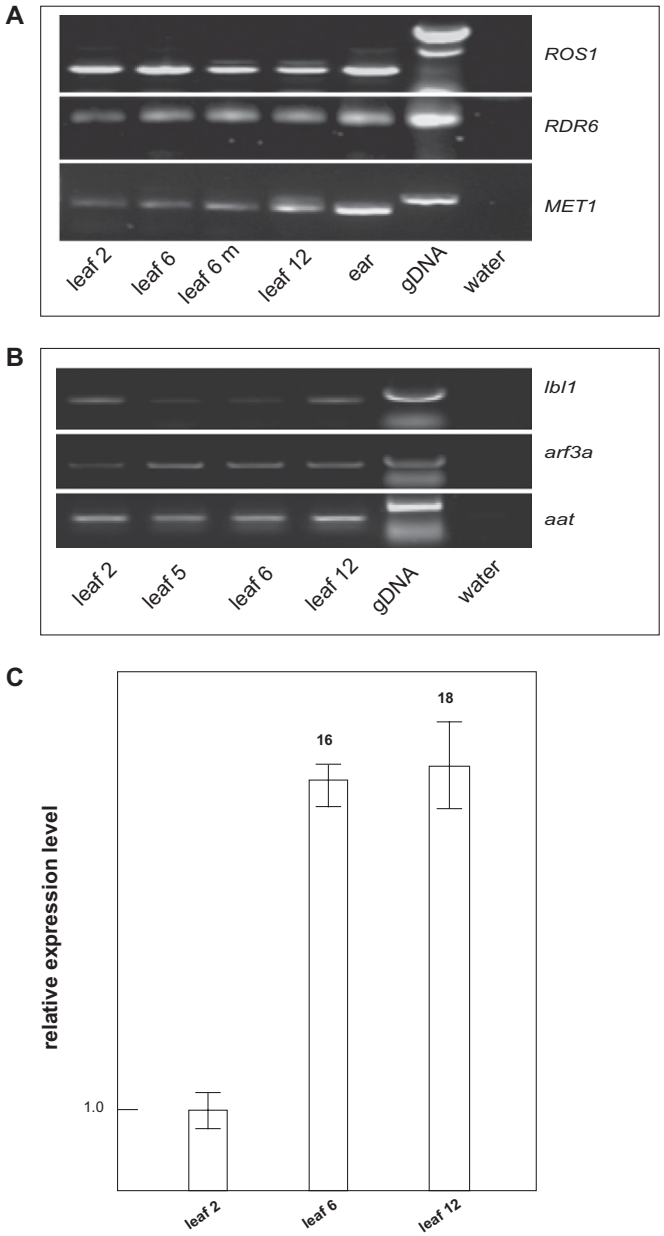

Fig. S6. RT-PCR analysis of gene expression. (*A*) mRNA levels of maize homologs of *ROS1*, *RDR6*, and *MET1* in various tissues of F1 plants. (*B*) mRNA levels of maize genes in plants carrying only active *MuDR* elements. (*C*) Quantitative PCR assay of the relative mRNA level of *ARF3* in leaves 2, 6, and 12 of plants carrying only active *MuDR*. Results were calculated as fold change normalized to the expression level of *aat* and then to the value of leaf 2, which was arbitrarily set at 1. Bars show SE.

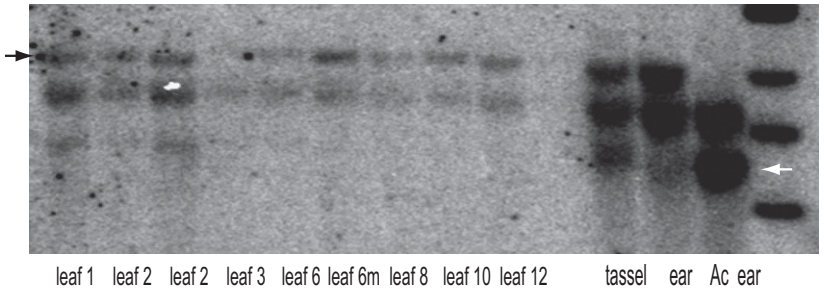

Fig. S7. Assay for functional transposase. *Mu1* methylation assay to determine the presence of functional transposase in various tissues. In the absence of transposase, the sites are methylated, resulting in a 2.1-kb fragment (left, black arrow). In the presence of transposase, HinfI sites in the terminal inverted repeats of *Mu1* at the reporter *a1-mum2* allele are unmethylated, resulting in a 1.3-kb fragment (right, white arrow).

Table S1. Primers used in the analysis

Primer	Sequence (5′ to 3′)
lblRTF1	TCACAAGGCCACAGAGGATAAAGA
lblRTR1	CACACGCGGCAACCACAG
ZmARF3F2	GCTGGAGGCATCGGAGGAACTG
ZmARF3R2	TACCGAACCATCAAACCGACACTG
ZmRDR6F2	AGGCAGGGGGACATAAAGGAGAG
ZmRDR6R2	ATGGCAAAGAGGGCAGAGTGGT
AGO7F4	GGTGGTGGAGCTGTCGTGTTAC
AGO7R4	GGAGGTCTGTTCATCTGAGAG
ZmMet1F1	ATGGGCGATTGAATACGAAGAGC
ZmMet1R1	GAGATGCAACTGCCAAACGGAAGG
ZmRos1F1	AGAAATGCAGGCTCAGAAAGTCAG
ZmRos1R1	TCGGGCTATCCATCCTCGTC
Aexon2F3	AGGCAGAGTACAAGTACCTACCG
mudrAexon2R8	ACCCTTACAGTATCCAACGTATCTT
aatF1	ATGGGGTATGGCGAGGAT
aatR1	TTGCACGACGAGCTAAAGACT
ACTINF	GATGATGCGCCAAGAGCTG
ACTINR	GCCTCATCACCTACGTAGGCAT
copiaF	CGATGTGAAGACAGCATTCCT
copiaR	CTCAAGTGACATCCCATGTGT
TIRAR	AGGAGAGACGGTGACAAGAGGAGTA
TIRAUTRR	ACTGGAGCGACGGGTGCTCGGCT
5′AflankF1	CAGAAGTACTCGTTGATGTCG
5′AflankR1	GGAAGAAGCTGCTCCTGTG
TIRAmF6	TYAGGGAAYTGGAGYGAYGGGTG
TIRAR3	GCCGAACCAGAGAGCATTTA
DrintF1	AAGGAAATGGYTAGTGAAGAAAAT
DrintR1	TTTTCTRCRCTCTATTTCTCT